In the isothermal case ($\gamma = 1$) $\omega(k, t)$ has a power-law dependence on the time:

$$\omega(k, t) = C_1 t^{\alpha_1} + C_2 t^{\alpha_2},$$

where $\alpha_{1,2} = \frac{1}{2} \pm \sqrt{(\frac{1}{4} - c_0^2 k^2)^{1/2}}$ and C_1, C_2 are constants. When α is complex-valued, $C_1 = \bar{C}_2$. In the isothermal case the motion is unstable, and the amplitude growth depends on the wavelength.

If we express the growth of the perturbations in terms of the relative compression ρ/ρ_0, we have

$$(\Delta\rho/\rho)/(\Delta\rho/\rho)_0 \leqslant (\rho/\rho_0)^{(1/4)(2-\gamma)} < (\rho/\rho_0)^{1/4},$$

because for real gases $1 \leq \gamma \leq 2$.

LITERATURE CITED

1. S. A. Kholin, "Stability analysis of the motion of a compressible gas," Zh. Prikl. Mekh. Tekh. Fiz., No. 6 (1965).

PROPAGATION OF FINITE-AMPLITUDE PRESSURE PERTURBATIONS IN A BUBBLING VAPOR – LIQUID MEDIUM

V. E. Nakoryakov, B. G. Pokusaev,
N. A. Pribaturin, and I. R. Shreiber

UDC 532.593:532.529

The investigation of the propagation of pressure perturbations in a liquid saturated with vapor bubbles has produced two different models describing this process. In [1] the wave evolution process is analyzed from the point of view of a thermodynamic-equilibrium model, in which the characteristic sound velocity is calculated in the form [2]

$$c_+ = \mu r p_0 / \left(B\rho_1 T_0 (c_{p_1} T_0)^{1/2}\right),$$

where p and T are the pressure and temperature of the medium, ρ is the density, c_p is the specific heat, r is the latent heat of phase transition, B is the gas constant, and μ is the molecular weight. We use the indices 1 and 2 everywhere to designate the liquid and the vapor respectively, and the index 0 for the unperturbed state. However, it is inferred from experiments [3-5] that the gas dynamics of a vapor–liquid medium with a bubble structure must be formulated on the basis of a nonequilibrium approach. A model has been proposed in [6] for the propagation of pressure disturbances with allowance for the unsteady behavior of the heat and mass transfer at the bubble–liquid phase interface during the transmission of the pressure pulse. As the characteristic velocity in this model we adopt the "frozen" sound velocity c_0, the value of which can be determined from the expression

$$\frac{1}{c_0^2} = \frac{(1-\varphi_0)^2}{c_1^2} + \frac{\varphi_0 (1-\varphi_0)\rho_1}{\gamma p_0},$$

in which φ_0 is the initial vapor content and γ is the adiabatic exponent for the vapor. The experiments reported in [5] show that the model used in [6] for the heat transfer between a vapor bubble and a liquid well describes the dynamics of bubbles for an arbitrary variation of the external conditions (pressure or temperature). The same experiments also show that the behavior of bubbles in a pressure wave is strongly mirrored in the structure and evolution of the waves. It was observed earlier [4] that under definite conditions the evolution of a pressure perturbation in a liquid containing vapor bubbles can be affected not only by interphase heat and mass transfer, but also by nonlinear and dispersion effects, which are typical of a bubbling gas–liquid medium [7].

Novosibirsk. Translated from Zhurnal Prikladnoi Mekhaniki i Tekhnicheskoi Fiziki, No. 3, pp. 84-90, May-June, 1982. Original article submitted April 6, 1981.

For the description of the evolution of a finite-amplitude pressure wave propagating in one direction in a bubbling vapor–liquid medium we have previously [6] derived an equation that has the following form in the majority of situations of practical importance:

$$\frac{\partial \Delta p}{\partial t} + c_0 \frac{\partial \Delta p}{\partial x} + \frac{\gamma+1}{2\varphi_0 \rho_0 c_0} \Delta p \frac{\partial \Delta p}{\partial x} - \nu \frac{\partial^2 \Delta p}{\partial x^2} + \beta c_0 \frac{\partial^3 \Delta p}{\partial x^3} = - m \frac{a_1^{1/2}}{R_0} \int_0^t \frac{\partial \Delta p / \partial t'}{(t-t')^{1/2}} dt', \tag{1}$$

where Δp is the instantaneous pressure perturbation, a is the thermal diffusivity, $m = 3\gamma p_0 c_{p_1} \rho_1 T_0 / 2\pi^{1/2} \rho_2^2 r^2$; $\beta = \varkappa R_0^2 / 6\varphi_0 (1-\varphi_0)$; $\nu = 2\nu_1 \varkappa / 3\varphi_0 (1-\varphi_0) + \gamma R_0 c_0^2 \varkappa / 2c_1$ are, respectively, the dispersion parameter and the effective viscosity of the medium associated with the viscosity ν_1 of the liquid and the acoustic radiation from a pulsating bubble of radius R_0, and $\varkappa = 1/(1 + c_0^2/c_1^2)$.

The integral term in (1) describes relaxation effects associated with unsteady heat and mass transfer between the vapor bubble and the surrounding liquid. An equation similar to (1), but with an exponential integrand, has been obtained in [8] for the description of relaxation effects in the propagation of a signal in a liquid containing gas bubbles.

The relative contributions of nonlinearity, dispersion due to dynamic effects associated with the oscillations of the vapor bubbles, dissipation associated with the effective viscosity of the medium, and the relaxation process to the evolution of the pressure perturbation in a vapor–liquid medium can be estimated by reducing Eq. (1) to dimensionless form. For the length scale we use a characteristic length l_0 of the initial perturbation, and for the time scale the ratio l_0/c_0. We refer the instantaneous pressure perturbation to the intensity of the initial perturbation Δp_0. Then Eq. (1) can be written, after suitable transformations, in the dimensionless variables $\tau = c_0 t \sigma / l_0$, $\xi = x\sigma/l_0$, $p^* = \Delta p/\Delta p_0$ as follows:

$$\frac{\partial p^*}{\partial \tau} + \frac{\partial p^*}{\partial \xi} + \mathrm{M} p^* \frac{\partial p^*}{\partial \xi} - \frac{\mathrm{M}\sigma}{\mathrm{Re}} \frac{\partial^2 p^*}{\partial \xi^2} + \frac{\partial^3 p^*}{\partial \xi^3} = - W \mathrm{M}^{1/2} \int_0^\tau \frac{\partial p^* / \partial \eta}{(\tau - \eta)^{1/2}} d\eta. \tag{2}$$

The parameters $\sigma = l_0 (u_0/\beta c_0)^{1/2}$, $\mathrm{Re} = u_0 l_0 / \nu$ characterize the dispersion and dissipation effects typical of a liquid containing gas bubbles [7]. The amplitude u_0 of the initial velocity perturbation is related to the pressure perturbation Δp_0 as $u_0 = (\gamma+1) c_0 \Delta p_0 / 2\gamma p_0$. The parameter for the integral term $W = [(\gamma+1)/2] \times \mathrm{Ja}(3\sigma/8\pi\varphi_0 \mathrm{Pe} \mathrm{M}^3)^{1/2}$ accounts for the rate of heat and mass transfer between the vapor bubbles and the liquid [5, 6] ($\mathrm{Ja} = \rho_1 c_{p_1}/T_0 \Delta\rho_2 r$ is the Jakob number, $\mathrm{Pe} = u_0 l_0 / a_1$, $\mathrm{M} = u_0/c_0$, and ΔT_0 and Δp_0 are related through the Clausius–Clapeyron equation). The main contribution to the dimensionless group W is from the number Ja, which represents a modified phase-transition criterion $K = r/c_{p_1} \Delta T_0$ [9].

An analysis of Eq. (2) shows that in the asymptotic case ($W \to 0$) (2) goes over to the Burgers–Korteweg–de Vries equation, which describes, for example, the evolution of a pressure wave in a bubbling gas–liquid medium [7]. According to the conclusions of this paper, the shape of the evolving perturbation depends on the ratio between the parameters σ and Re. In the low-dissipation case ($\sigma/\mathrm{Re} < 0.1$) for $\sigma > \sigma_*$ the initial perturbation decays into solitons, and for $\sigma < \sigma_*$ it is transformed into a wave packet (σ_* is the critical value of the similarity criterion, calculated according to [10]). In the case of appreciable dissipation, in this case due to acoustic losses, the wave evolution process will also depend on the value of the parameter Re [7]. Estimates show that for the majority of vapor–liquid media the acoustic losses do not exceed the losses due to heat and mass transfer at the outer boundary of the vapor bubble. Thus, in a vapor–liquid medium with very slow interphase heat- and mass-transfer processes (such as a steam–water mixture at high initial pressures or cryogenic systems) the wave states typical of gas–liquid systems can exist [7]. For large values of W (steam–water mixture at low pressures or liquid metals) the dissipation associated with the effective viscosity of the medium and dynamic effects can be disregarded in Eq. (2), so that only the integral term is left in (2). The linear version of this equation admits an analytical solution [6]. In this case the powerful action of the heat- and mass-transfer relaxation process will cause rapid decay of the initial perturbation. Thus, by contrast with a gas–liquid medium, the behavior of the pressure waves in a liquid containing vapor bubbles must be determined mainly by the similarity parameters σ and W.

We have studied experimentally the evolution of wave states in a vapor–liquid medium in the saturated state over a wide range of values of the dimensionless groups σ and W for the purpose of determining the boundaries of influence of the heat- and mass-transfer relaxation process, inertial effects, and nonlinearity on the wave dynamics. The experiments were conducted in a shock tube [5]; the primary pulse was generated by bursting a diaphragm separating the working section from the high-pressure chamber. The parameter σ was varied by varying the amplitude and duration of the initial pressure pulse, and W was varied by varying the

TABLE 1

Test No.	Working medium	$p_0\cdot10^{-5}$, Pa	T_0, °K	$R_0\cdot10^3$, m	$\Delta p_0\cdot10^{-5}$, Pa	l_0, m	M	W	σ	L, m	$\Delta p_m\cdot10^{-5}$, Pa
1	Water	1,3	380,4	1,5	0,26	0,112	0,18	0,47	9,5	0,34	0,052
2	»	1,8	390,1	1,5	1,35	0,162	0,67	0,13	26,5	0,34	0,51
3	»	5,25	426,2	1,4	0,13	0,098	0,02	0,65	2,5	0,4	0,026
4	»	5,1	425,2	1,4	1,47	0,107	0,26	0,097	10,5	0,425	0,34
5	»	5	424,6	1,4	4	0,188	0,72	0,04	31,6	0,415	0,68
6	Freon-12	13,2	326,6	1	0,2	0,081	0,014	0,12	2,9	0,7	0,08
7	»	13	325,7	1	1,9	0,105	0,13	0,021	11,9	0,445	1,51
8	Freon-21	2,1	302	1,2	3,66	0,212	1,63	0,013	55,2	0,415	2,27
9	Water	1,9	391,2	1,5	0,15	—	0,071	0,72	—	0,485	0,085
10	»	4,9	424	1,4	0,49	—	0,09	0,24	—	0,765	0,35
11	Freon-12	6,85	300	1,3	0,72	—	0,096	0,034	—	0,915	0,68
12	Freon-21	1,85	298,4	1,2	0,68	—	0,34	0,059	—	0,46	0,6
13	Freon-12	13,6	327,5	1	5,06	—	0,35	0,0094	—	0,485	5,5
14	»	7,05	301	1,3	5,05	—	0,67	0,0062	—	0,915	6,4
15	Freon-21	1,7	296	1,2	2,76	—	1,5	—	—	0,17	9,8
16	Freon-12	1	243	2	6	—	5,64	—	—	0,62	~30
17	Nitrogen	1	78	3	1,5	—	1,28	—	—	0,16	~20
18	Water	1	373	2	1	—	0,9	—	—	0,43	4

thermophysical properties of the liquid. This was done by increasing the static pressure for a steam–water mixture and changing to liquids having a high thermal resistance: Freon 21 and Freon 12, permitting W to be varied in the experiments from 10^{-2} to 1. For identical values of π_* ($\pi_* = p_0/p_*$, where p_* is the pressure at the critical point of the substance) and σ the value of W was the same for the steam–water and vapor–Freon media. This fact evinces the possibility of modeling the process of evolution of a perturbation in a steam–water medium with a high initial pressure by a vapor–Freon medium existing at experimentally more accessible pressures.

Our primary concern in the experiments was to maintain the working medium in the saturated state and to obtain a homogeneous bubbling mixture. Accordingly, the working section of the shock tube was placed in a double thermostat with electric heaters. The wall temperature of the section was maintained equal to the temperature of the working medium at the given pressure within 0.5°C error limits. The working section with a length of 1.8 m was assembled from blocks of stainless steel tubing with an inside diameter of 0.052 m and a wall thickness of 0.008 m. Vapor bubbles were generated at artificial vaporization centers situated below the working section. The average bubble radius in the experiments was varied according to the working conditions from $1.1 \cdot 10^{-3}$ to $1.6 \cdot 10^{-3}$ m. The average volume vapor content was maintained constant in all the experiments and was of the order of 1%. The variation of R and φ along the height of the working section due to the presence of hydrostatic pressure turned out to be small, since all the experiments were conducted at above-atmospheric initial pressures. To facilitate rapid replacement of the burst disk (diaphragm) we developed a special bursting mechanism capable of operating without breaking the seal of the equipment [5]. The length of the high-pressure chamber was varied up to a maximum of 2 m.

The instantaneous pressure in the pulses transmitted through the vapor–liquid medium was measured with LKh 610 piezoelectric transducer probes. The analog signal received from the transducers was recorded on a Schlumberger MP 5521/2 tape recorder and then processed on an M-6000 digital computer. The details of the procedure for measuring the parameters of the medium and processing the experimental data are described in [5].

Using the similarity parameters W and σ, we can represent all the results in the form of a map of the various wave structures, as in Fig. 1, which shows the most characteristic wave profiles, corresponding to times of the order of $5 \cdot 10^{-3}$ sec from the initial entry of the signal into the medium. The interval $\sigma > 10^2$ corresponds to initial perturbations of the "step-function" type. All the data on the state of the vapor–liquid medium and the initial pressure perturbation are summarized in Table 1, in which L is the distance from the entry into the medium and Δp_m is the maximum pressure in the wave. The value of σ_* is calculated for each experiment and on the average is of the order of 10.

The map clearly exhibits the regions in which heat- and mass-transfer, inertial, and nonlinear effects are manifested in different degrees. The forms of the evolving perturbations differ accordingly.

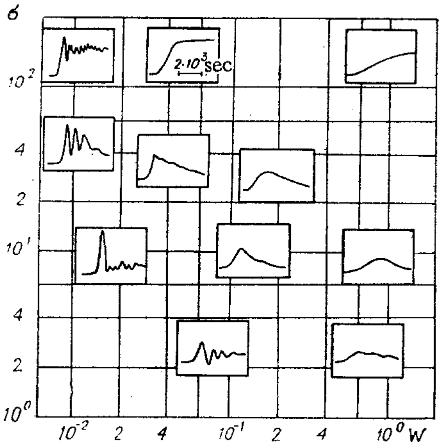

Fig. 1

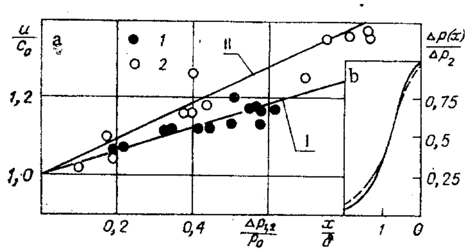

Fig. 2

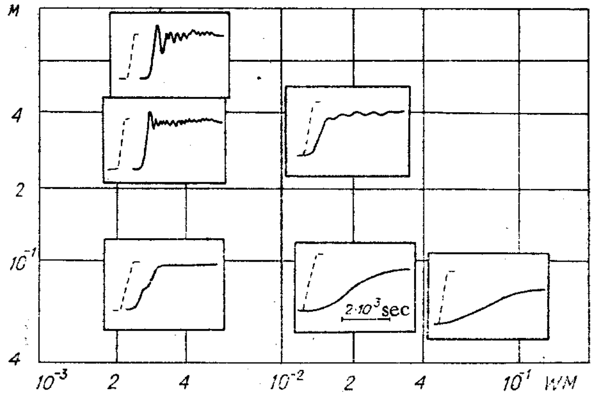

Fig. 3

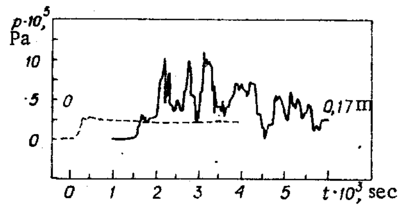

Fig. 4

Thus, for large values of W (W ~ 1, tests 1 and 9 in Table 1) the predominant influence of the relaxation process of interphase heat and mass transfer results in considerable broadening of the shock front and the formation of a rapidly decaying bell-shaped perturbation in the case of a wave of finite duration. An increase in the nonlinearity of such a medium, corresponding to an increase of σ and a decrease of W (test 2), only slightly increases the steepness of the wave front. With a further decrease in W as a result of, for example, an increase in the static pressure of a steam–water medium (tests 3-5), nonlinear and dispersion effects begin to emerge, as are typical of a "cold" liquid containing gas bubbles. However, the action of these effects is significant only in the initial stage of wave evolution. Subsequently, the influence of the relaxation process tends to attenuate and broaden the "soliton" perturbation and causes the pulsations to vanish after the shock front, which eventually smears out. In the event of a weak influence of interphase heat and mass transfer ($W < 10^{-1}$) wave structures similar to those in a gas–liquid medium [7] are formed (tests 6-8, 11, 14). A triangular initial perturbation is converted, depending on the parameter σ, either into solitary waves (tests 7 and 8) or into an oscillating perturbation similar in profile to a wave packet (test 6). In the case of an initial perturbation in the form of a "step" a shock wave with a monotonic (test 11) or oscillating (test 14) profile is formed over the entire length of the working section, depending on the nonlinearity parameter M.

The behavior of the pressure waves in a low-dissipation vapor–liquid medium, namely their velocity and profile, are consistent with the main conclusions drawn from an analysis of the Burgers–Korteweg–de Vries equation. For example, the experimental and analytical results on the propagation velocity of solitons (points 1) and shock waves (points 2) as a function of their intensity are compared in Fig. 2a. It is seen that the experimental data are well generalized by the standard [7] equations for the velocity of solitons $u = c_0[1 + (\gamma + 1)\Delta p_2/6\gamma p_0]$ (line I) and shock waves $u = c_0[1 + (\gamma + 1)\Delta p_1/4\gamma p_0]$ (line II), where Δp_2 is the amplitude of the solitary wave and Δp_1 is the postshock pressure. The experimental results shown here were obtained in Freon 12 saturated with vapor bubbles at $p_0 = 6.6 \cdot 10^5$ Pa. The profile of the resulting perturbation (test 7, solid curve) is compared in Fig. 2b with the soliton profile calculation according to the relation [7, 10] (dashed curve): $\Delta p(x) = \Delta p_2 \operatorname{sech}^2(x/\delta)$, where the half-width δ of the soliton is specified in the form

$$\delta = \left(\frac{4\gamma}{\gamma+1}\right)^{1/2} \frac{R_0}{\varphi_0^{1/2}} \left(\frac{p_0}{\Delta p_2}\right)^{1/2}.$$

The influence of the rate of interphase heat and mass transfer on the structure and evolution of shock waves can be traced in Fig. 3, which, as in Fig. 1, shows the wave profiles for characteristic times of the order of $5 \cdot 10^{-3}$ sec. The dashed curves in Fig. 3 show the scale for the initial pressure perturbation and its profile.

An intense phase-transition process, characterized by values of the parameter $W \sim 1$, produces rapid broadening of the shock front. The wave in this case is highly transient (test 9), and its profile is determined mainly by the process of heat and mass transfer between the vapor bubbles and the surrounding liquid. With a decrease in the parameter W at a constant intensity of the initial profile (test 10) the shock smearing effect is slowed down somewhat. At these distances the wave profile becomes increasingly steeper, and with an increase in the wave intensity (test 12) dispersion effects begin to emerge in connection with the inertia of the additional mass of the vapor bubbles. However, the ever-increasing influence of interphase heat and mass transfer tends to smooth the initially oscillating wave (test 12).

A further decrease in the rate of the transfer process at the vapor bubble–liquid interface results in the formation of a quasistationary shock wave over the entire length of the working section. Its profile is determined mainly by nonlinear and inertial effects, as are typical of gas–liquid media [7], and can be either monotonic (test 11) or oscillating (tests 13 and 14). The value of the dimensionless group $MW \leq 6 \cdot 10^{-3}$ can in this case be taken as the criterion for the onset of a quasistationary wave structure, and the quantity $M \sim 0.3$ as the criterion of transition from a monotonic to an oscillating wave profile.

In conclusion we note that for large intensities of the initial perturbation ($M > 1$) a severalfold amplification of the initial shock wave was observed in the experiments. A typical profile of the resulting wave is shown in Fig. 4, and the characteristics of the medium and initial perturbation are given in Table 1 (test 15). Similar amplification effects have been observed previously in cryogenic liquids [11] (tests 16 and 17) and in the case of wave reflection from a barrier in a steam–water medium [4] (test 18). The amplification of the initial perturbation can be attributed to the breakup of bubbles in the wave [11] or to a decrease in the compressibility of the vapor–liquid medium in the final stage of collapse of the vapor bubbles and cannot be described within the scope of the model in question.

Thus, the results of our investigations of the dynamics of pressure waves in a bubbling vapor–liquid medium evince the strong influence of interphase heat and mass transfer on the profile and evolution of the perturbation. The results can be used to predict the behavior of waves in media with various thermophysical properties over a wide range of static pressures.

LITERATURE CITED

1. V. E. Nakoryakov, V. V. Sobolev, and I. R. Shreiber, "Finite-amplitude waves in two-phase systems," in: Wave Processes in Two-Phase Systems [in Russian], ITF Sib. Otd. Akad. Nauk SSSR, Novosibirsk (1975).
2. L. D. Landau and E. M. Lifshits, Continuum Mechanics [in Russian], Gostekhizdat, Moscow (1954).
3. N. I. Semenov and S. I. Kosterin, "Results of a study of the sound velocities in moving gas–liquid mixtures," Teploénergetika, No. 6 (1964).
4. S. S. Kutateladze, V. E. Nakoryakov, and B. G. Pokusaev, "Experimental investigation of wave processes in gas- and vapor-liquid media," in: Two-Phase Momentum and Heat-Mass Transfer, Vol. 1, Hemisphere, Washington-New York (1979).
5. B. G. Pokusaev, A. V. Korabel'nikov, and N. A. Pribaturin, "Pressure waves in a liquid containing vapor bubbles," in: Wave Processes in Two-Phase Media [in Russian], ITF Sib. Otd. Akad. Nauk SSSR, Novosibirsk (1980).
6. V. E. Nakoryakov and I. R. Shreiber, "Model of the propagation of disturbances in a vapor–liquid mixture," Teplofiz. Vys. Temp., 17, No. 4 (1979).
7. V. V. Kuznetsov, V. E. Nakoryakov, et al., "Propagation of disturbances in a gas–liquid mixture," Akust. Zh., 23, No. 2 (1977).
8. V. G. Gasenko, V. E. Nakoryakov, and I. R. Shreiber, "The Burgers–Korteweg–de Vries approximation in the wave dynamics of gas–liquid systems," in: Nonlinear Wave Processes in Two-Phase Media [in Russian], ITF Sib. Otd. Akad. Nauk SSSR, Novosibirsk (1977).
9. S. S. Kutateladze, Fundamentals of the Theory of Heat Transfer [in Russian], Atomizdat, Moscow (1980).
10. Yu. A. Berezin and V. I. Karpman, "Nonlinear evolution of perturbations in a plasma and other dispersive media," Zh. Éksp. Teor. Fiz., 51, No. 5 (1966).

11. A. A. Borisov, B. E. Gel'fand, et al., "Amplification of shock waves in a liquid containing vapor bubbles," in: Nonlinear Wave Processes in Two-Phase Media [in Russian], ITF Sib. Otd. Akad. Nauk SSSR, Novosibirsk (1977).

STRONG ACTION OF A STRONGLY UNDEREXPANDED LOW-DENSITY JET ON A PLANE OBSTACLE

É. N. Voznesenskii and V. I. Nemchenko

UDC 532.525.6.011.5

One of the fundamental characteristics of the strong action of a freely expanding gas jet or a strongly underexpanded gas jet on an obstacle is the pressure distribution on the surface. For a phenomenological description of the interaction and development of engineering computation methods, it is also useful to know the shape of the shock which occurs here. Investigation of the interaction between a strongly underexpanded gas jet and a plane obstacle parallel to the jet axis should be extracted as a separate problem. All the results published in the literature [1-5] for the analysis of this problem have substantially been obtained in dense jets. Examples of specific pressure distributions on an obstacle are presented in [1-3], and in addition, methods are given for an approximate computation of the magnitude of the induced pressure. As a rule, different modifications of the Newton method or the method of tangential wedges are recommended. According to estimates [2, 4], the accuracy of such computations is not more than satisfactory and drops rapidly downstream. A search for other means of solving the problem, particularly for modeling the phenomena in wind tunnels with subsequent representation of the results in criterial form, is of interest. Such an approach is used in [4, 5], where similarity criteria are constructed for the dimensionless representation of the shock and the extension of the pressure distribution to a plate parallel to the jet axis on the basis of similarity theory and the criterial characteristics of a strongly underexpanded jet derived in [6], and appropriate empirical dependences are proposed for dense jets.

Data of an experimental investigation of an analogous problem, performed on low-density jets, are presented below.

The conditions characterizing the jet outflow (air is the working gas) are the following: stagnation pressure $p_0 = 4.13 \cdot 10^4$–$6.67 \cdot 10^4$ Pa, stagnation temperature $T_0 = 395$–780°K, pressure in the working chamber $p_\infty = 1.33$–13.3 Pa, degree of flow expansion $N = p_0/p_\infty = 0.5 \cdot 10^4$–$4 \cdot 10^4$ for nozzle Mach numbers determined without taking account of the boundary layer, $M_a = 1.0$–3.92. The distance $h = H/r_a$ between the model surface and the jet axis, expressed in nozzle exit section radii r_a varied between 4–20. Under conditions of the experiment $Re_L = Re_*/N^{1/2}$, where Re_* is the Reynolds number computed with respect to the critical gas parameters and the diameter of the nozzle critical section, varied between 14 and 160, i.e., was substantially less than the value $Re_L \sim 10^3$–10^4 characteristic for [1-5]. Therefore, according to the classification of the flow structure in a jet by the Reynolds numbers Re_L [7, 8], the investigation represented occupies a domain between the domain of interaction with a diffuse jet surface on the one hand, and a jet with a turbulent mixing layer on the other, and corresponds to the case of interaction of a completely laminar jet with an obstacle when the effects of viscosity and rarefaction still do not reach that part of the jet core in every case, by which the strong load on the obstacle is defined for the range of values of h presented.

Included in the paper are data of just those experiments in which the influence of a hanging shock or the external pressure on the measurement results is not detected.

1. The experiments were performed in a vacuum wind tunnel, for which the diagram of the working section is shown in Fig. 1a. The gas goes through the leak 1 to the mixing chamber 2 equipped with a labyrinth type resistance heater and closed by a cooled screen, then escapes through the cooled nozzle 3 in the strong underexpansion mode into the working chamber where the cooled model 5 is mounted on the plotting board 4

Moscow. Translated from Zhurnal Prikladnoi Mekhaniki i Tekhnicheskoi Fiziki, No. 3, pp. 90-98, May-June, 1982. Original article submitted March 23, 1981.

